INSTITUT D'AERONOMIE SPATIALE DE BELGIQUE

3 - Avenue Circulaire
B - 1180 BRUXELLES

AERONOMICA ACTA

A - N° 204 - 1979

Temperature, molecular nitrogen concentration and turbulence in the lower thermosphere inferred from incoherent scatter data

by

D. ALCAYDE, J. FONTANARI, G. KOCKARTS, P. BAUER and R. BERNARD

BELGISCH INSTITUUT VOOR RUIMTE-AERONOMIE

3 - Ringlaan
B - 1180 BRUSSEL

FOREWORD

The paper "Temperature, molecular nitrogen concentration and turbulence in the lower thermosphere inferred from incoherent scatter data" will be published in Annales de Géophysique, 35, 1979.

AVANT-PROPOS

L'article "Temperature, molecular nitrogen concentration and turbulence in the lower thermosphere inferred from incoherent scatter data" sera publié dans les Annales de Géophysique, 35, 1979.

VOORWOORD

De tekst "Temperature, molecular nitrogen concentration and turbulence in the lower thermosphere inferred from incoherent scatter data" zal in het tijdschrift Annales de Géophysique, 35, 1979, verschijnen.

VORWORT

Die Arbeit "Temperature, molecular nitrogen concentration and turbulence in the lower thermosphere inferred from incoherent scatter data" wird in Annales de Géophysique, 35, 1979 herausgegeben werden.

TEMPERATURE, MOLECULAR NITROGEN CONCENTRATION AND TURBULENCE IN THE LOWER THERMOSPHERE INFERRED FROM INCOHERENT SCATTER DATA

by

D. ALCAYDE[1], J. FONTANARI[1], G. KOCKARTS[2], P. BAUER[3] and R. BERNARD[3]

(1) Centre d'Etude Spatiale des Rayonnements
Boîte Postale 4346
F - 31029 Toulouse Cedex, France.

(2) Institut d'Aéronomie Spatiale
3 Avenue Circulaire
B - 1180 Bruxelles, Belgique.

(3) Centre de Recherche en Physique de l'Environnement terrestre et planétaire
38-40 rue du Général Leclerc
F - 92131 Issy-les-Moulineaux, France.

Abstract

Incoherent scatter data gathered over almost one solar cycle (1967 - 1975) in the height range 95 - 150 km at 45° North, provide an opportunity to study and to modelize long term variations of the daytime neutral temperature and the N_2 concentration. The main features identified in this study are the absence of solar cycle effects in the temperature variations around 100 km, a minimum in the daily mean temperature profile around 100 km moving upwards from summer to winter with consequently a reversal in the seasonal trend above and below 100 km, an increase in the daily mean N_2 density around 100 km for solar maximum conditions, and a gradual change from a pure semi-annual variation at 95 km to a dominant seasonal variation above 100 km in the daily averaged N_2 concentration. The temperature data are used to compute the vertical eddy diffusion coefficient between 95 and 120 km for equinox and solstice conditions. Large seasonal variations are apparent in the daily averaged eddy diffusion coefficients.

Résumé

Les données de diffusion incohérente obtenues entre 95 et 150 km à 45° Nord sur une période de l'ordre d'un cycle d'activité solaire (1967 - 1975) offrent une possibilité d'étudier et de modéliser les variations à long terme de la température diurne moyenne et de la concentration en azote moléculaire. Cette étude met en évidence l'absence d'effet du cycle solaire sur la température aux environs de 100 km. De plus le profil vertical de la moyenne diurne de la température passe par un minimum aux environs de 100 km. Ce minimum se déplace vers le haut entre l'été et l'hiver, ce qui entraîne un renversement de la variation saisonnière au-dessus et au-dessous de 100 km. On observe également un accroissement de la moyenne diurne de la concentration en N_2 lors du maximum d'activité solaire. Cette moyenne diurne est caractérisée par une variation semiannuelle à 95 km qui devient une variation annuelle au-dessus de 100 km. Finalement, les données de température sont utilisées pour calculer une distribution verticale du coefficient de diffusion turbulente entre 95 et 120 km pour des conditions d'équinoxe et de solstice. De grandes variations saisonnières apparaissent dans la moyenne diurne des coefficients de diffusion turbulente.

Samenvatting

Gegevens, bekomen door incoherente verstrooïngsmetingen over praktisch een volledige zonnecyclus (1967-1975) op een hoogte van 95 tot 150 km op 45°NB, bieden de mogelijkheid trage temperatuursveranderingen te bestuderen van de neutrale atmosfeer overdag evenals de concentratie der moleculaire stikstof en ervan een model te ontwerpen. Vooreerst stelt men in deze studie vast dat de temperatuur op 100 km geen invloed ondervindt van de zonnecyclus. Uit de analyse deze verticale temperatuursprofielen blijkt dat de minimumwaarde van de gemiddelde temperatuur overdag onveranderd blijft en in de buurt van 100 km gelegen is. Bij de seizoenwisseling van zomer naar winter verplaatst het zich een weinig opwaarts met als gevolg een tegengesteld temperatuursverloop boven en onder de 100 km. Men stelt eveneens een toename vast van de moleculaire stikstofconcentratie bij maximale zonneactiviteit. Het daggemiddelde, gekenmerkt door een halfjaarlijkse schommeling op 95 km, gaat geleidelijk een jaarlijkse schommeling vertonen wanneer men de 100 km overschrijdt. Uiteindelijk wordt uit de temperaturen het verticaal verloop bepaald van de turbulente diffusiecoëfficient tijdens de eveningen en het solstitium en dit voor een hoogtebereik van 95 tot 120 km. Hierbij stelt men grote waardeverschillen vast.

Zusammenfassung

Inkohärente Streuungsdaten erreicht zwischen 95 und 100 km Höhe für 45°N Breite über eine Periode von ungefähr ein Sonnenzyklus (1967-1975) erlauben eine Modellisierung der Variationen der mittleren täglichen Temperatur und der Stickstoffkonzentration. Es gibt kein Sonnenzyklus-effekt auf der Temperatur in der Umgebung von 100 km. Die mittlere tägliche Temperatur erreicht einen Minimumwert in der Umgebung von 100 km. Dieses Minimum bewegt sich nach oben zwischen Sommer und Winter und dafür beobachtet man einen Umkehr der Jahreszeitvariation oberhalb und unterhalb 100 km. Der tägliche Mittelwert der N_2 Konzentration steigt während eines Maximum der Sonnenaktivität. Dieser Mittelwert hat einen halbjährlichen Gang auf 95 km Höhe und einen jährlichen Gang oberhalb 100 km. Schliesslich benützt man die Temperaturdaten um eine senkrechte Ausbreitung des Turbulenzkoeffizienten zwischen 95 und 120 km für Äquinoktium und Solstitium zu berechenen. Grosse Jahreszeitvariationen werden für die tägliche Mittelwerte des Turbulenzkoeffizienten enthalten.

1. INTRODUCTION

The identification of the main physical processes acting in the thermosphere is of prime interest for the understanding of the thermodynamical coupling between the upper and lower parts of the atmosphere and of the global distribution of the atmospheric constituents.

The lower thermosphere is actually a transition region where wave and tidal energies originating from the lower atmosphere are converted into heat through various dissipation processes (viscosity, ion drag...) and where turbulent mixing ceases to allow diffusive separation of the atmospheric species.

As yet, the observations performed in this region are still scarce, since it lies out of reach of in situ satellite measurements and since rocket experiments are widely scattered in space and time.

The incoherent scatter technique is certainly the one single technique which has allowed a continuous monitoring of this part of the atmosphere. Short term variations such as tides or gravity waves have been extensively studied (e.g. Wand, 1969; Bernard and Spizzichino, 1971; Salah and Wand, 1974; Fontanari and Alcaydé, 1974; Mathews, 1976; Harper, 1977; Vidal Madjar, 1978). The mean state of the lower thermosphere and its long term variations, on another hand, require a thorough investigation after the initial studies performed by Waldteufel (1970), and by Alcaydé, Bauer and Fontanari (1974).

The purpose of this paper is to present and model an extensive series (1967-1975) of N_2 density and temperature measurements gathered respectively over the altitude ranges 95-110 km and 95-150 km above the French incoherent scatter station of Saint-Santin (45°N). The interpretation of these data leads to a determination of the eddy diffusion coefficient versus altitude and season.

2. DATA CHARACTERISTICS

The incoherent scatter technique provides a determination of various plasma parameters (concentration, electron and ion temperatures, ion velocity) and for low altitudes (95-110 km) a determination of the ion neutral collision frequency (Dougherty and Farley, 1963; Waldteufel, 1969; Tepley and Mathews, 1978).

Since thermal equilibrium between the ions and the neutrals prevails in the lower thermosphere, the thermal structure can be established from the ion temperature (T_i) measurements. Daily mean temperatures have been plotted on Fig. 1 versus time over the period 1967-1975 for altitudes varying between 95 and 150 km. Each point is a weighted average corresponding to one day of experiment. The weight of each individual data point is determined by its statistical error. The measurements can only be made during daytime when the E region of the ionosphere is well developed and, therefore, the averages must be understood as daytime averages. However, previous studies (e.g. Bernard, 1974; Salah, 1974) have shown that semi-diurnal variations dominate in the lower thermosphere, so that in a first approximation the daytime averages can be equated to diurnal averages. The error bars plotted in Fig. 1 are statistical errors determined from the statistical errors affecting each individual measurement.

Also plotted in Fig. 1 is the resulting model which includes seasonal, semi-annual and solar cycle effects. It will be described in the following section.

The well known seasonal variation (summer maximum) is clearly visible down to 105 km. The 100 km altitude is almost an isothermal level at about 200 K. A trend for a reversal of the seasonal effect (winter maximum) is visible at 95 km. It should be also noted that in the 95 to 105 km region the temperature is almost constant on the mean and that large temperature gradients develop upwards.

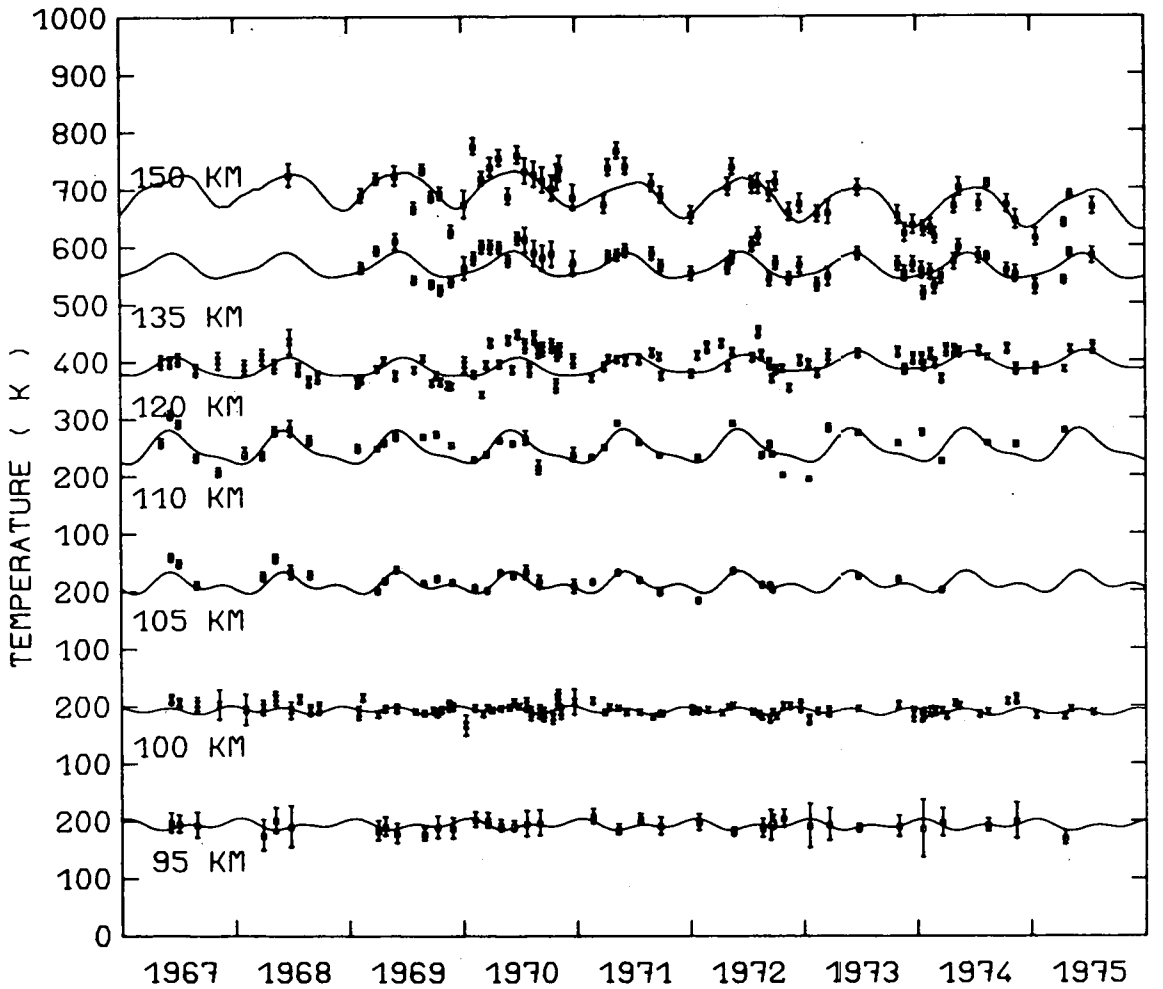

Fig. 1.- Long term observations of temperature above Saint-Santin between 95 and 150 km. Each data point corresponds to a statistical diurnal average of the observations. The solid lines represent the fit of data with solar flux dependence and seasonal variation. Note that the scale is progressively shifted up to 105 km.

Similarly Fig. 2 shows daily mean molecular nitrogen concentrations plotted versus time between 1967 and 1975 for altitudes varying between 95 and 110 km. They have been derived from ion neutral collision frequency measurements (Waldteufel, 1969).

One noticeable feature is the abrupt change in the accuracy of the data in early 1969. This is due to a change in the sensitivity of the incoherent scatter equipment of Saint-Santin. Collisional effects on the incoherent spectrum become progressively negligible around 110 km and upwards. Therefore, caution must be exerted before interpreting the trends observed at this height.

As for the temperature, the molecular nitrogen concentrations have been modelled through a least square fitting of the data. The results of the modelling is shown in Fig. 2 and will be discussed in section 3.

Note that previous studies (Waldteufel, 1970; Alcayde et al., 1974) find a confirmation in this larger data basis. Namely the density variations exhibit a summer minimum at 100 km. The similar minimum is present at all heights. In addition to that, semi-annual variations dominate at 95 km and leave the way to annual variations at greater heights.

3. TEMPERATURE AND MOLECULAR NITROGEN MODELLING

3.1. Fourier analysis

A Fourier analysis has been performed on the whole set of the diurnally averaged temperature and N_2 data. At each altitude the temperature and N_2 data are weighted by the inverse of the square of their error bar, and are respectively fitted with the relations

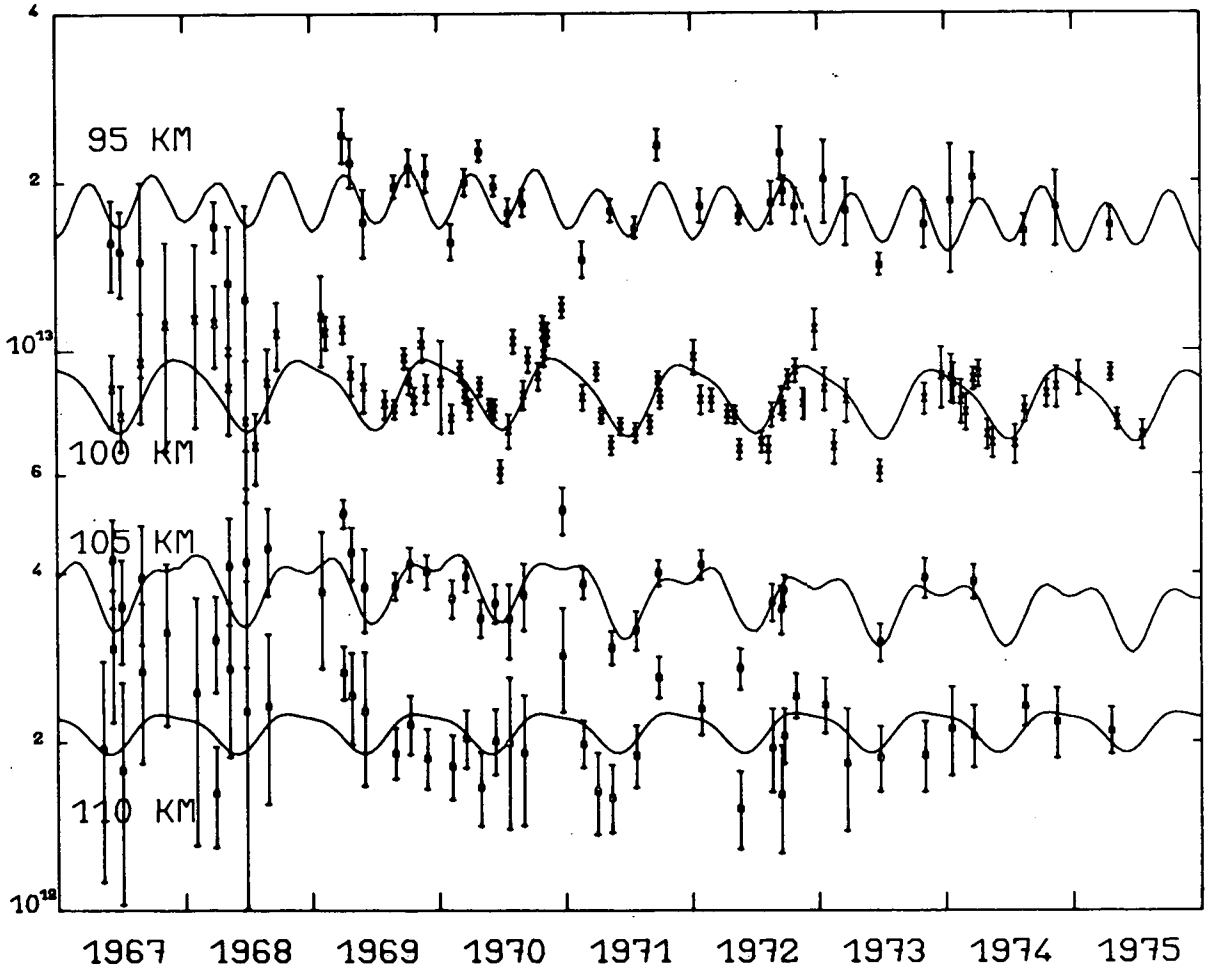

Fig. 2.- Same as Fig. 1 for molecular nitrogen concentration.

$$T = T_o + a\,\bar{F}_{10.7} + \sum_{i=1}^{2} \left\{ A_i \cos\left[\frac{2\pi i}{365} (d - \phi_i) \right] \right\} \quad (1)$$

$$\log n(N_2) = A_o + a\,\bar{F}_{10.7} + \sum_{i=1}^{2} \left\{ A_i \cos\left[\frac{2\pi i}{365} (d - \phi_i) \right] \right\} \quad (2)$$

where $\bar{F}_{10.7}$ is the solar decimetric flux expressed in 10^{-22}W m^{-2} Hz^{-1} and averaged over three solar rotations centered on the day d of observation, T_o is the mean temperature, A_o is the mean value of the decimal logarithm of the molecular nitrogen concentration $n(N_2)$ in cm^{-3}, a is the solar flux dependence, A_i and ϕ_i are respectively the amplitude and the day of maximum of the annual (i = 1) or semi-annual (i = 2) variation. A statistical error is computed for each parameter A_i and ϕ_i, taking into account the experimental errors and the goodness of the fit. Such a procedure gives the information about the actual influence of each parameter on the quality of the fit. The standard deviations between the fits and the data are of the same order of magnitude as the mean experimental error (15 K for the temperatures for example). The global fit is shown as a continuous lines in Figs. 1 and 2 for the temperature and the N_2 concentration. The solar flux dependence is clearly evidenced for the temperature at 150 km where the mean decrease of the solar decimetric flux from 150 to 70 between 1967 and 1975 leads to a corresponding decrease of 40 K. For the molecular nitrogen concentration a positive solar flux effect is noticeable between 95 and 105 km, but not at 110 km. The solar flux dependence of the temperature and the N_2 concentrations will be further specified when the whore result of the fit is discussed.

On Fig. 3 temperature data are plotted for each altitude versus the day number in the year, the whole set of temperatures being gathered on a single year. The continuous line represents the fit according to relation (1) with a constant solar decimetric flux of 125 and using the coefficients listed in Table 1. The 95 and 100 km levels

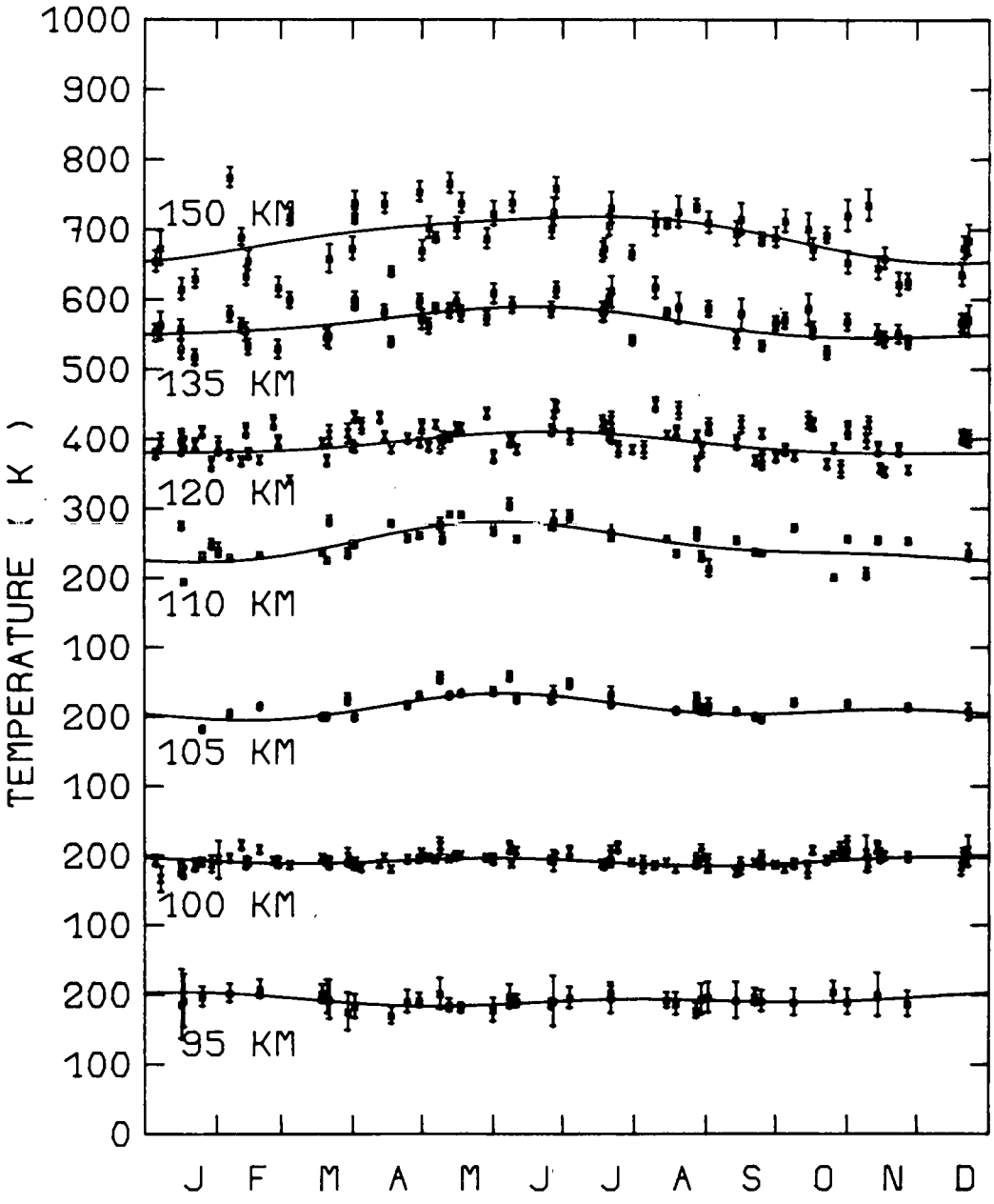

Fig. 3.- The whole set of temperature data is gathered on one year. The solid lines correspond to a fit with a constant solar decimetric flux of 125 x 10^{-22} W m^{-2} Hz^{-1}. Scale shifted as in Fig. 1.

TABLE 1 : Coefficients of equation (1) issued from the Fourier analysis on mean diurnal temperature data in the 95-150 km range, over the years 1967 to 1975.

			annual variation		semi-annual variation	
Altitude	Mean value	Flux dependence	amplitude	phase	amplitude	phase
Z (km)	T_o (K)	a $K(W\ m^{-2}\ Hz^{-1})^{-1}$	A_1 (K)	ϕ_1 (days)	A_2 (K)	ϕ_2 (days)
95	190.1	2.49×10^{-2}	5.76	- 9	5.50	204
100	184.5	6.45×10^{-2}	1.86	36	5.23	155
105	211.8	1.58×10^{-4}	12.4	173	10.52	150
110	249.8	-1.49×10^{-3}	25.6	166	9.12	144
120	407.8	-1.29×10^{-1}	15.5	172	3.98	175
135	553.2	9.00×10^{-2}	21.3	159	4.97	176
150	626.3	5.06×10^{-1}	32.3	175	5.87	247

show a nearly constant mean diurnal temperature without any significant seasonal variation and with a noteworthy weak scatter of the points. The seasonal variation appears at 105 km and then increases with altitude, showing a rather large amplitude at 110 km.

Fig. 4 displays the seasonal variations of the molecular nitrogen, using equation (2) and the coefficients given in Table 2. At 95 km, the variation is essentially semi-annual, with maxima around the equinoxes. At higher levels, an annual variation is superimposed on the semi-annual one, leading to minimum concentrations at the summer solstice, and a broad maximum between the autumn and spring equinoxes.

Figs. 5a,5b, 6a and 6b display the altitude variation of the coefficients in equation (1) and (2) resulting from the Fourier analysis of temperatur and N_2 concentration data. Fig. 5a shows the amplitudes and days of maximum (so called phase) of the annual and semi-annual variations of temperature from 95 up to 150 km altitude. As previously noted on Figs. 1 and 3, the amplitude of the annual component is very weak at the lower levels, and increases with increasing altitude, up to 30 K at 150 km. At 110 km, this annual amplitude reaches 26 K, which is larger than the values at the surrounding altitudes. This particular trend was noticed by Waldteufel (1970), on a limited set of data. Except for the 95 and 100 km levels, where its amplitude is very weak, the annual variation leads to a maximum near the summer solstice, throughout the 105 to 150 km altitude range. The amplitude of the semi-annual variation remains weak and nearly constant (5 K) for all the levels, with a slight increase at 105 km (10 K of amplitude). From 95 up to 135 km, the semi-annual component maximizes near the solstice, but the larger annual amplitude leads to a maximum of temperature at the summer solstice.

The dependence of temperature versus solar decimetric flux is shown on Figs. 5b. From 95 up to 135 km, the temperature is weakly

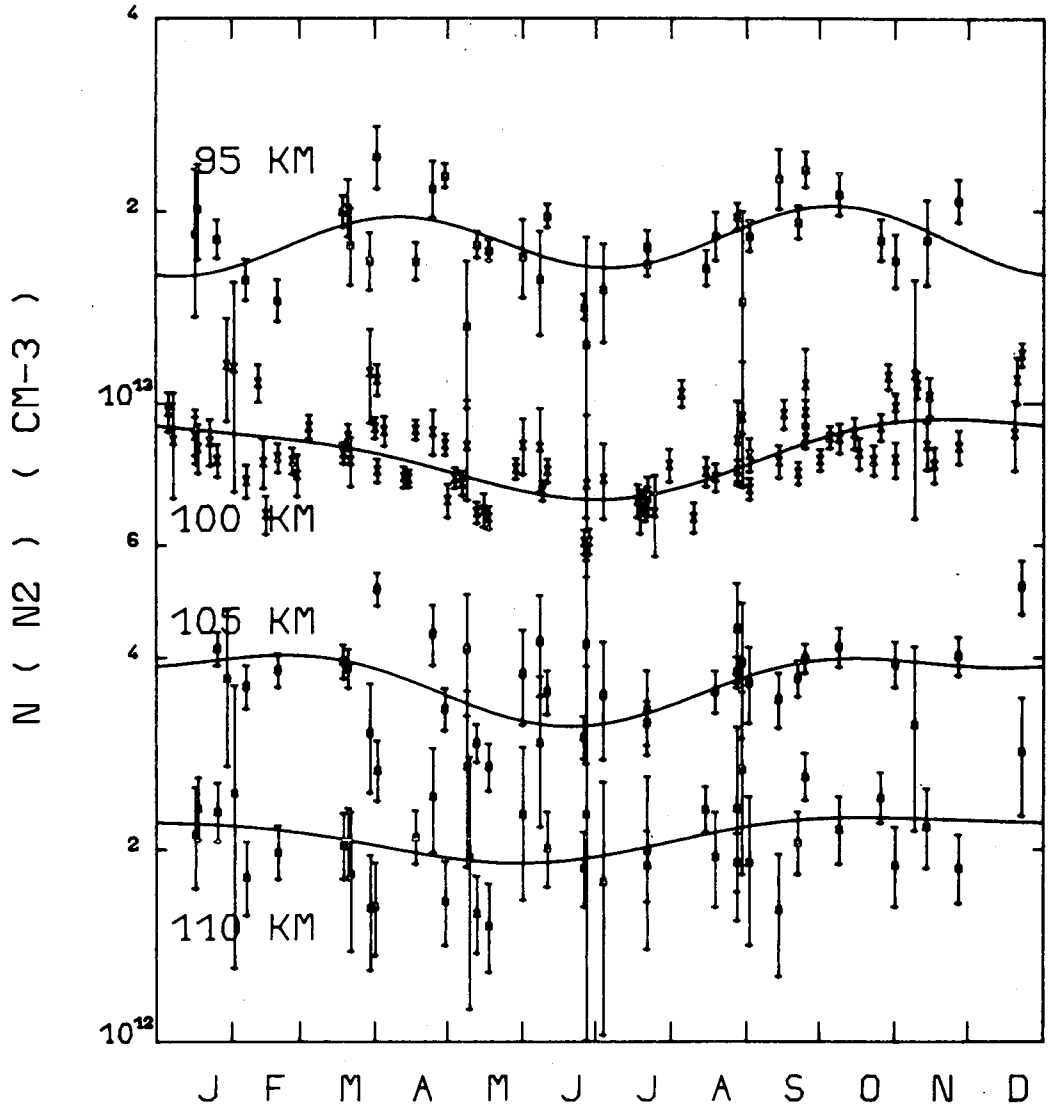

Fig. 4.- Same as Fig. 3 for molecular nitrogen concentration.

TABLE 2 : Coefficients of equation (2) issued from the Fourier analysis on decimal logarithm of mean diurnal N_2 concentration data, in the 95-110 km range, over the years 1967-1975.

			annual variation		semi-annual variation	
Altitude	Mean value	Flux dependence	amplitude	phase	amplitude	phase
Z (km)	A_o	a $(W\ m^{-2}\ Hz^{-1})^{-1}$	A_1	ϕ_1 (days)	A_2	ϕ_2 (days)
95	13.18	6.20×10^{-4}	1.1×10^{-2}	242	4.7×10^{-2}	97
100	12.88	3.10×10^{-4}	5.9×10^{-2}	353	1.4×10^{-2}	102
105	12.48	6.76×10^{-4}	4.6×10^{-2}	356	2.7×10^{-2}	78
110	12.32	-0.18×10^{-4}	3.4×10^{-2}	326	9.4×10^{-3}	65

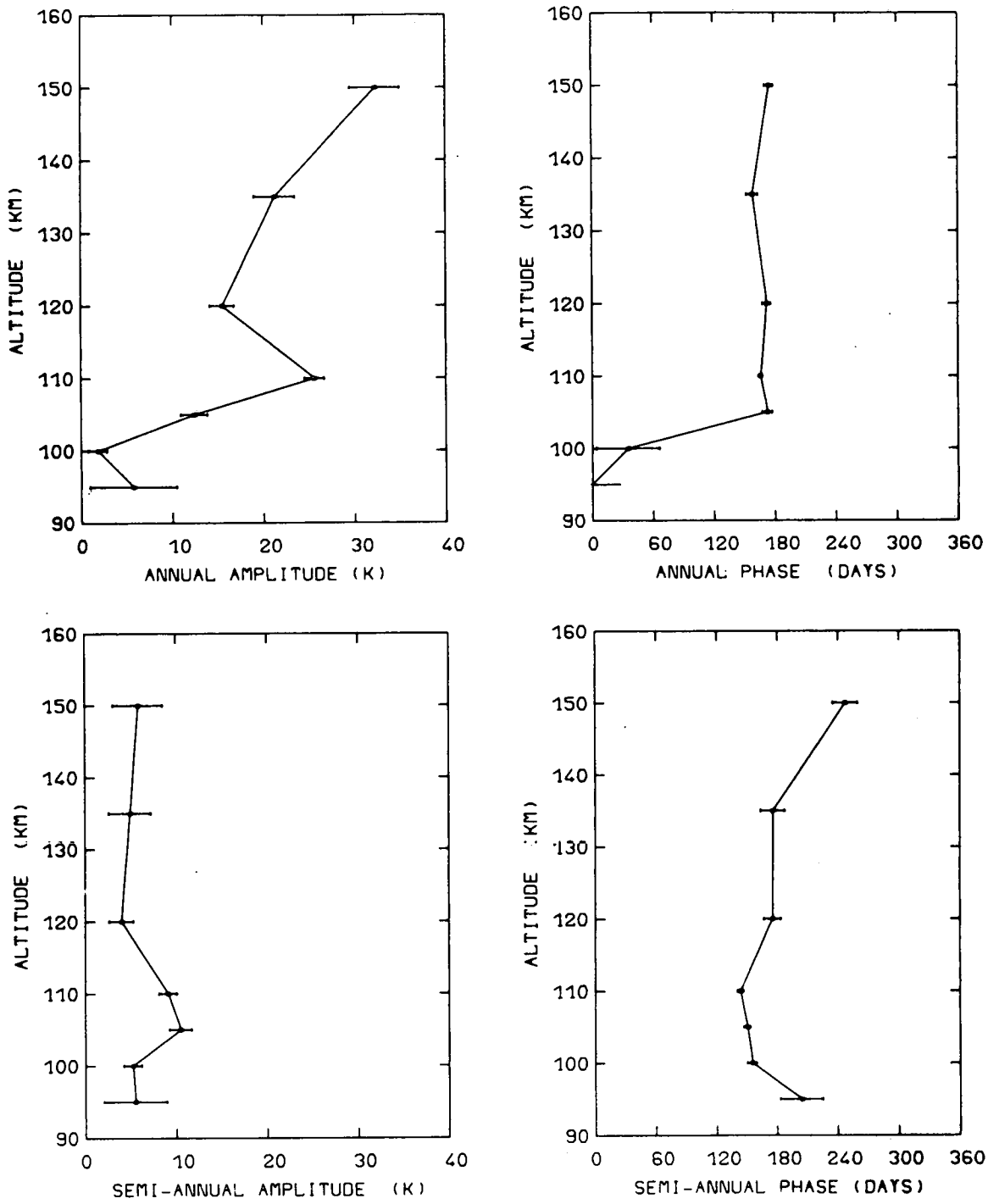

Fig. 5a.- Altitude dependence of the annual and semi-annual amplitude and phase of the temperature according to equation (1).

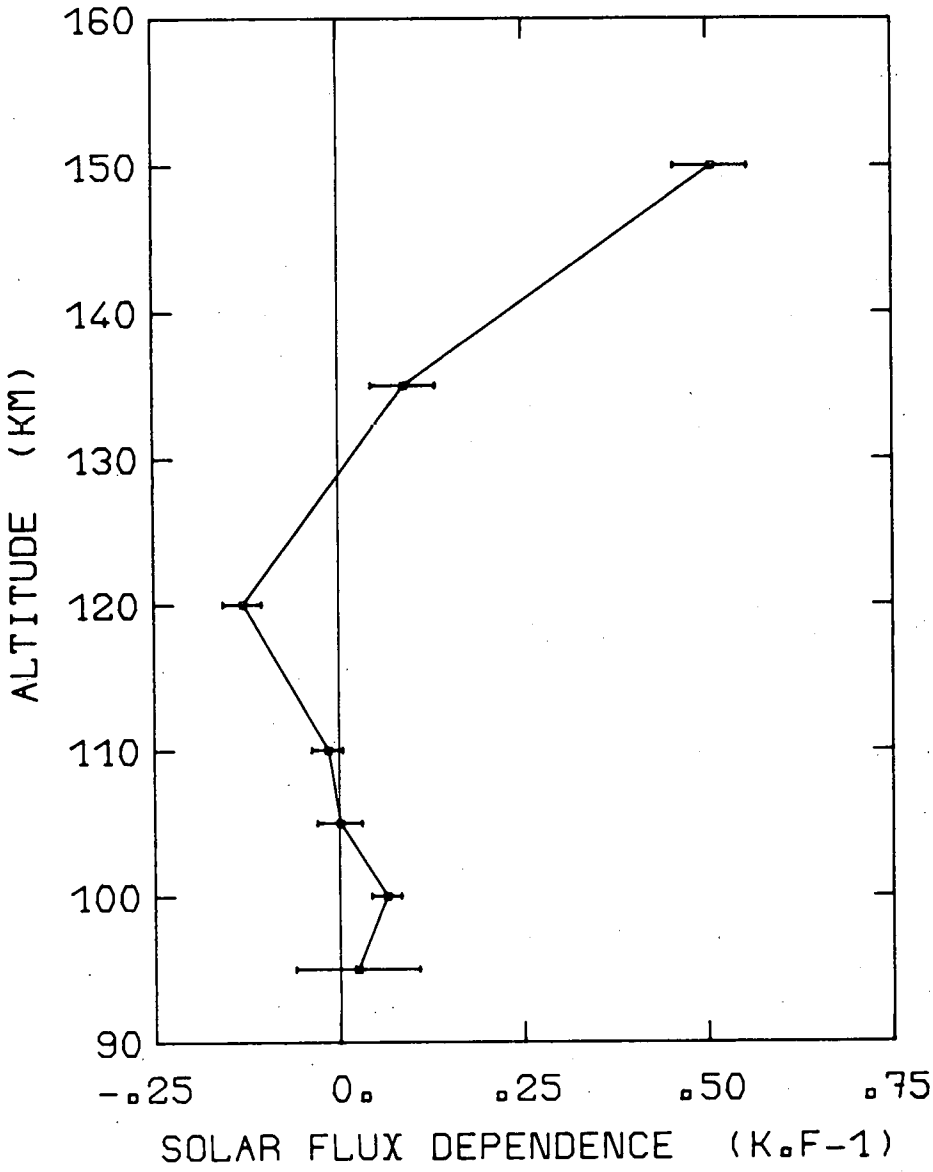

Fig. 5b.- Altitude dependence of the solar flux coefficient for the temperature given by equation (1).

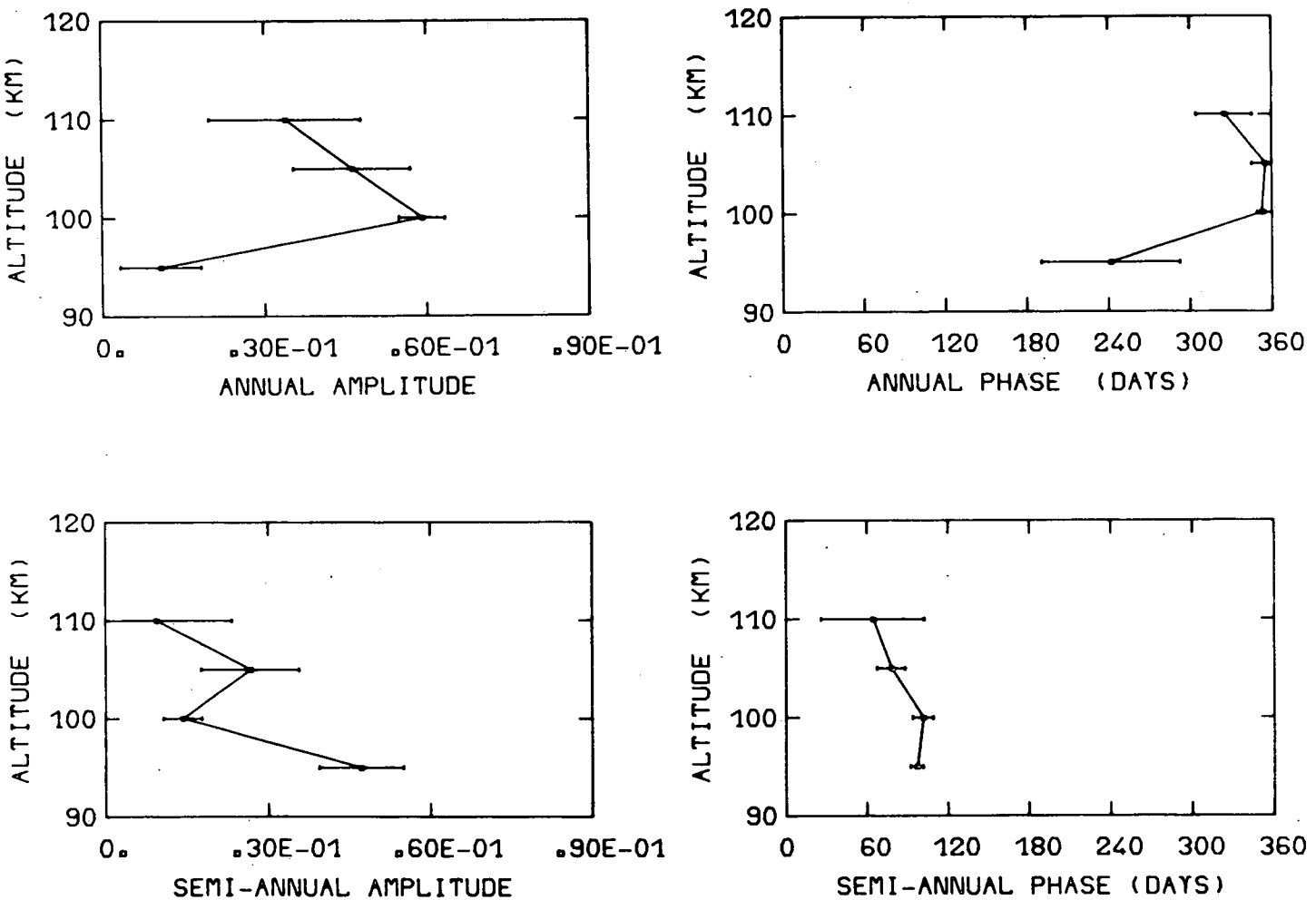

Fig. 6a.- Same as Fig. 5a for molecular nitrogen given by equation (2).

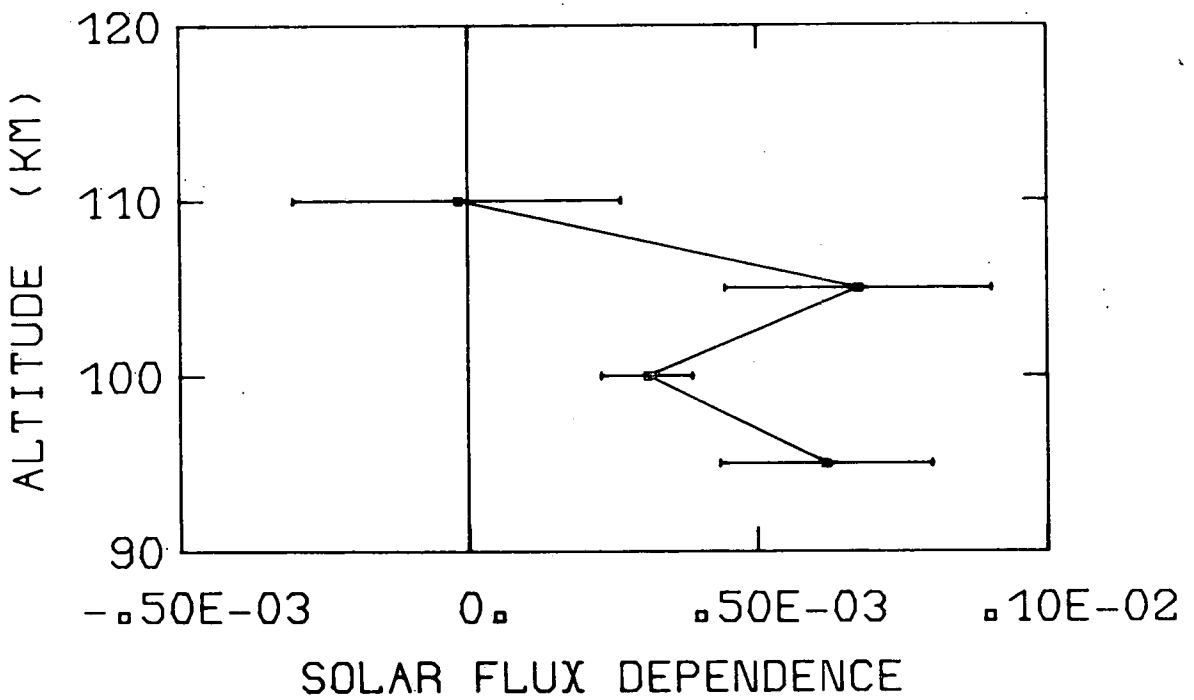

Fig. 6b.- Same as Fig. 5b for molecular nitrogen given by equation (2).

altered by solar flux changes. The negative value at 120 km is weak but implies a 13 K decrease in temperature for a 100 units (10^{-22}W m^{-2} Hz^{-1}) increase of the solar decimetric flux. At 150 km altitude, the dependence becomes positive and larger.

The results of the Fourier analysis applied to the decimal logarithm of N_2 concentrations in the 95 - 110 km altitude range are displayed on Fig. 6a and 6b. Fig. 6a shows the characteristics of the annual and semi-annual variations. At 95 km the amplitude of the annual component is very weak. It becomes larger at the upper levels, decreasing slowly from 100 km up to 110 km, while the day of maximum occurs approximatively at the winter solstices. The semi-annual variation, whose maxima occur approximately at equinoxes, is important at 95 km and negligible at 110 km, its amplitude decreasing with increasing height. The solar flux dependence, shown on Fig. 6b is roughly constant between 95 and 105 km and then decreases to zero at 110 km. At 95 km, a change of 100 units (10^{-22}W m^{-2} Hz^{-1}) in the $F_{10.7}$ index induces a 15% variation of the mean value (1.48×10^{13} cm^{-3}) of N_2 issued from the analysis. Such a variation may be compared with the amplitude of the seasonal effect which is of the same order of magnitude.

These results, established over approximatively one solar cycle data basis, allow us to confirm and to precise the indicative trends of the seasonal variations in the E region previously inferred by Waldteufel (1970), Waldteufel and Cogger (1971), Alcaydé et al. (1974) and Salah, Evans and Wand (1974) who studied Saint-Santin, Arecibo and Millstone Hill incoherent scatter data for maximum activity conditions.

3.2. Vertical temperature profiles (95 - 120 km)

The vertical temperature profiles in the 95-120 km altitude range (i.e. around and just above the mesopause) are very important as they result from the combined effects of solar heating and of the turbulent

and moleculer heat transfer. It is thus useful to characterize the seasonal behaviour by an analytical model of the vertical temperature profiles at equinoxes and solstices. In this respect, a fit of the temperature values for the chosen days, as issued from the long term modelling, was attempted.

The vertical distribution of the temperature between 95 and 120 km can be represented with a good accuracy by a quadratic variation, with a fourth-degree polynomial form :

$$T(z) = A_1 \left[1 + A_3 (z - A_2)^2 + A_4 (z - A_2)^4\right] \qquad (3)$$

The resulting coefficients of equation (3) are listed in Table 3 for each of the 4 days studied. On Fig. 7, the resulting fit is shown (continuous line) throughout the five points of each profile. The quality of the fit is very good, with a standard deviation of 7 K, to be compared with the mean error of 14 K of the individual temperatures. It can be observed that the mesopause, which will be defined here as the level where the minimum of temperature occurs, is higher (100 km) and broader in winter than in summer (less than 95 km), with an intermediate value at the equinoxes (97 km). Furthermore, the temperature minimum is larger for winter solstice (198 K) than for the other days (184 to 187 K). The altitude and amplitude of the temperature minima so observed, combined with weakly variable temperature at 120 km, lead to vertical temperature gradients near 120 km which are maximum in winter (27 K/km) and minimum in summer (14 K/km).

On Fig. 7 the dashed lines represent the profiles provided by the empirical model of Jacchia (1977), for the same conditions of geomagnetic (K_p = 2) and solar ($\bar{F}_{10.7} = 125 \times 10^{-22}$ W m^{-2} Hz^{-1}) activities. The agreement is rather good in the 95-110 km altitude range, except for the summer solstice. Substantial deviations appear nevertheless in the shape of the vertical temperature distribution, leading to systemat-

TABLE 3 : Coefficients of equation (3) obtained by fitting the long-term modelized temperature at the 95 - 100 - 105 - 110 - 120 km levels at the equinox and solstice times.

Day	A_1 (K)	A_3 (km^{-2})	A_4 (km^{-4})	A_2 (km)
Spring equinox	188.0	2.41×10^{-3}	-1.01×10^{-7}	98.8
Summer solstice	184.1	2.29×10^{-3}	-6.15×10^{-7}	94.4
Autumn equinox	185.8	1.97×10^{-3}	5.93×10^{-7}	98.0
Winter solstice	198.3	0.75×10^{-3}	2.63×10^{-6}	98.4

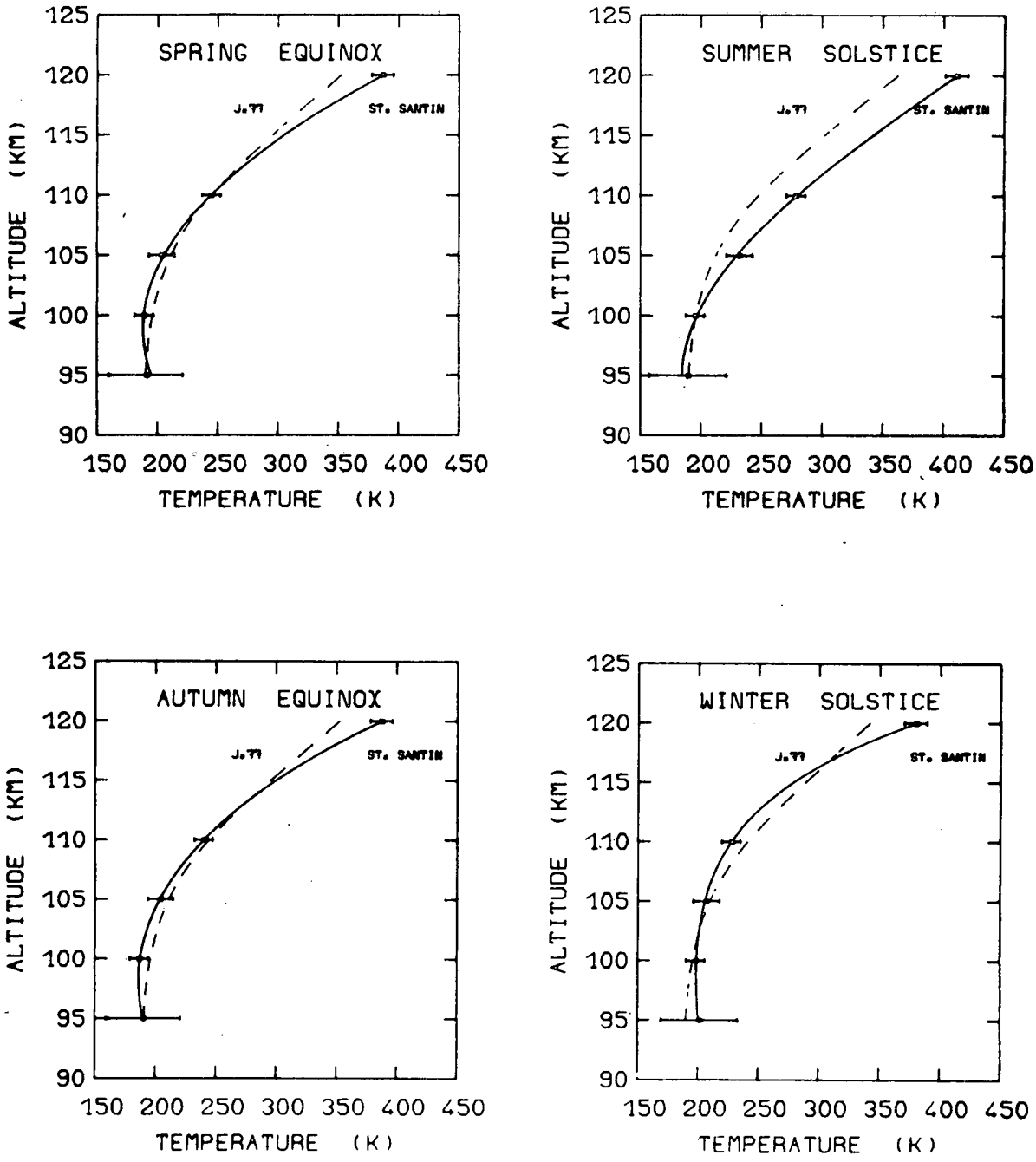

Fig. 7.- The seasonal fit of observed temperatures leads to characteristic values which are shown for $\overline{F}_{10.7}$ = 125 as a function of altitude. The error bars are computed from the uncertainties on the coefficients of equation (1). The full lines give the best fit of these points with equation (3). Jacchia's (1977) model is shown by the dashed lines.

ically underestimated temperature and vertical gradient at 120 km, and seasonal variations throughout the 95 - 120 km range.

The vertical temperature profiles according to equation (3) and Table 3, are then used to integrate the equation of mixing equilibrium, assuming a linearly varying mean molecular mass from 28.7 a.m.u. at 95 km to 27.3 a.m.u. at 110 km, in order to get the vertical decrease of the N_2 concentrations from the modelized value at 95 km up to 110 km. The vertical distributions of N_2 for the solstices and equinoxes are shown on Fig. 8 (continuous line) compared to the values provided at each height by the long-term modelling (equation (2), Table 2). The agreement is rather good, except at the 110 km level where the experimental values are larger than the calculated ones. Alcaydé, Bauer, Hedin and Salah (1978) pointed out the good agreement between Jacchia (1971) model and the incoherent scatter N_2 determination at St. Santin. Fig. 8 shows that the agreement is still rather good with the Jacchia (1977) model (dashed line) as well for the vertical profiles as for the mean concentrations.

Reasons for overestimating the molecular nitrogen concentrations at 110 km have been sought in two directions. Firstly one must note that the step from the measured ion neutral collision frequency to the molecular nitrogen concentration implies a knowledge of the relative abundance of the remaining atmospheric constituents. In the data reduction it has been assumed that molecular oxygen was the only other constituent of practical abundance with a mixing ratio of 20%. Above 95 km atomic oxygen, however, becomes progressively an important atmospheric constituent which could in principle affect the data reduction procedure. With an atomic oxygen concentration of 2×10^{11} cm^{-3} at 110 km (Philbrick, Faucher and Trzcinski, 1973) the molecular nitrogen concentration at 110 km is only reduced by 6%. This effect, therefore, can only be partly responsible for the overestimation of N_2 at 110 km.

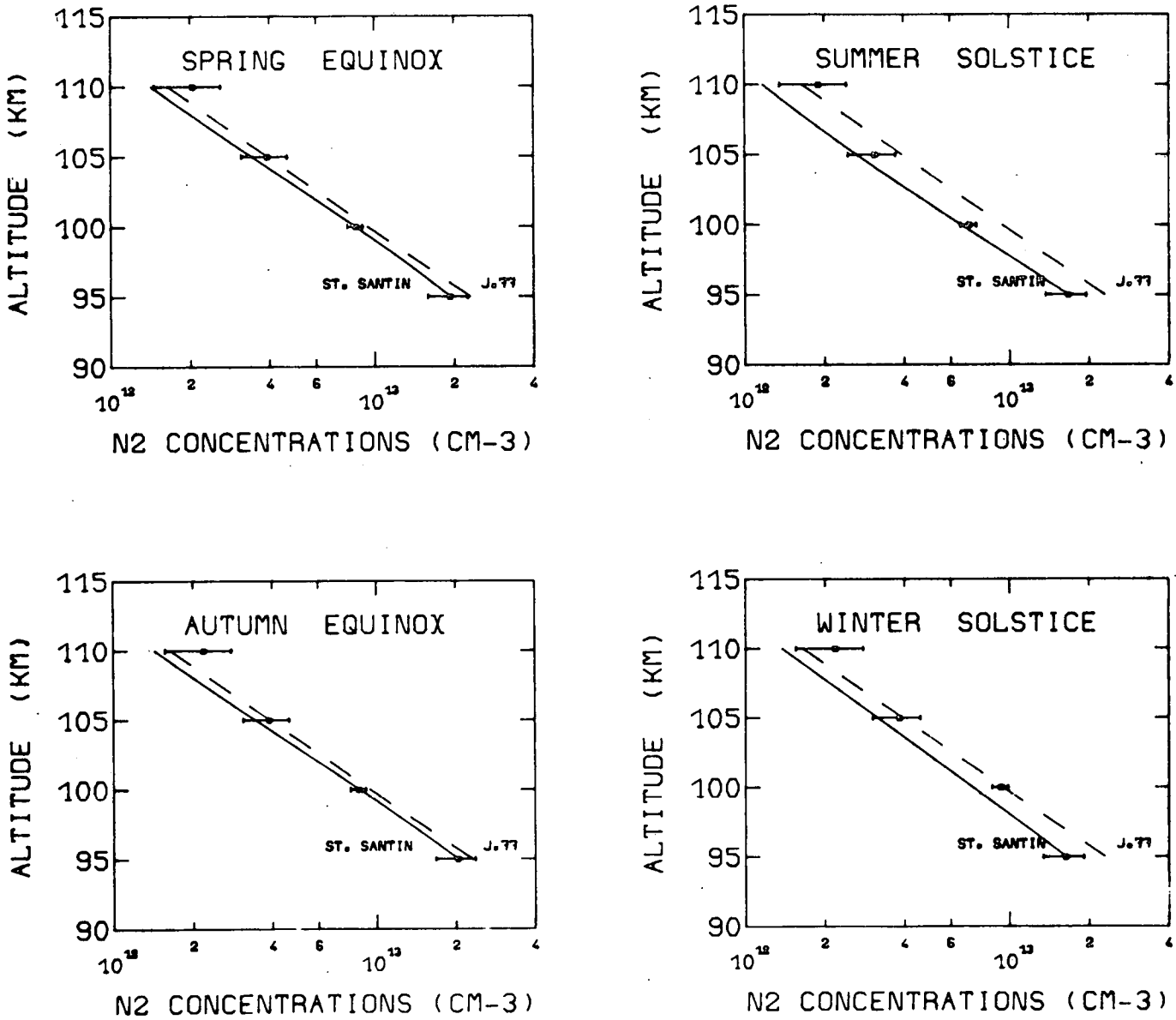

Fig. 8.- The seasonal fit of observed molecular nitrogen concentrations leads to characteristic values which are shown for $\overline{F}_{10.7}$ = 125 as a function of altitude. The error bars are computed from the uncertainties on the coefficients of equation (2). The full lines correspond to mixing distributions with the temperature profiles of Fig. 7 and the dashed lines represent Jacchia's (1977) values.

Another effect can result from the fact that the observing volume extends over an altitude range of approximately 4 km. Over this height range temperatures and densities can vary so that the average parameters obtained from the incoherent scatter spectra are not necessarily equal to the mean values. This effect was simulated theoretically and it appeared that the collision frequency tends to be enhanced by some 10% above the mean value, while the temperature remains approximately equal to its mean value.

The combination of these two effects can only explain an overestimation of the order of 15% instead of the 30% shown in Fig. 8. It appears, therefore, that caution must be exerted before using the collision data at 110 km and above.

4. APPLICATION TO EDDY DIFFUSION COEFFICIENTS

The transition region between the homosphere and the heterosphere is essentially dominated by the competition between turbulence and molecular diffusion. Although molecular diffusion coefficients can be computed from gas kinetic theory combined with laboratory data, the physical situation is less clear for the eddy diffusion coefficients associated with small-scale motions which prevent atmospheric constituents from diffusive separation in the Earth's gravitational field.

Assuming that turbulence is associated with a downward heat transport, Johnson and Wilkins (1965a, 1965b) deduced an upper limit on eddy diffusion in the mesosphere and lower thermosphere. Such a turbulent downward heat transport is actually introduced to eliminate the excess heat input which cannot be transported by molecular heat conduction or by infrared emission. Averaging the heat excess over time and over the Earth's surface, Johnson and Gottlieb (1970) computed a worldwide average eddy diffusion coefficient required to

maintain continuity in the heat budget between 60 and 120 km altitude. Hunten (1974) pointed out that downward eddy conduction may be balanced by phenomena such as gravity waves which can contribute to heating by their dissipation. Johnson (1975) questionned, however, Hunten's argument in a detailed discussion of the Richardson criterion for growth or maintenance of turbulence and he concluded that turbulence does not deposit more heat in the thermosphere than it removes from it. This controversial problem has been recently reanalyzed by Izakov (1978) for several planets. Using estimates of the flux Richardson number, Izakov (1978) concluded that turbulent cooling of the thermosphere prevails on Venus and on the Earth. On Jupiter, turbulence heats the thermosphere while on Mars turbulent heating of the thermosphere dominates for a quiet troposphere and turbulent cooling prevails for a disturbed troposphere.

Observations of chemical releases (Blamont and Barat, 1967; Zimmerman and Trowbridge, 1973) allow also a determination of eddy diffusion coefficients in the lower thermosphere. Using wind data Zimmerman and Murphy (1977) have shown that a large seasonal variation occurs in the eddy diffusion coefficient for altitudes below 90 km and for high latitudes. Teitelbaum and Blamont (1977) analyzed variations of kinetic energy involved in wind regimes during the night between 90 and 110 km and concluded that the atmosphere at mid-latitude remains turbulent up to 105 km between dusk and 22.00 LT whereas the turbopause height decreases to 95 km during the second part of the night.

Using the diurnally averaged temperature distributions and the molecular nitrogen concentrations obtained from incoherent scatter data, an analysis of the thermal balance can lead to an estimate for diurnally averaged eddy diffusion coefficients between 95 and 120 km above Saint-Santin. The energy balance equation averaged over a 24 hours period can be written as

$$\frac{\partial E}{\partial z} = P - L \qquad (4)$$

where P and L are respectively the heating rate and the cooling rate averaged over 24 hours. The downward vertical heat flux E is given by

$$E = -\lambda \frac{\partial T}{\partial z} - K \rho c_p \left(\frac{\partial T}{\partial z} + \frac{g}{c} \right) \qquad (5)$$

where λ is the molecular heat conduction coefficient taken from Banks and Kockarts (1973), T is the temperature at height z, ρ is the total atmospheric density, c_p is the atmospheric specific heat at constant pressure, g is the acceleration due to gravity and K is the unknown eddy diffusion coefficient. The first term in equation (5) is the downward heat flux due to molecular heat conduction and the second term represents the downward heat flux resulting from turbulent heat conduction.

With help of equation (5), integration of (4) from height z' to infinity leads to

$$K = \frac{\int_{z'}^{\infty} (P - L)\, dz - \lambda\, \partial T/\partial z}{\rho c_p \left(\frac{\partial T}{\partial z} + \frac{g}{c_p} \right)} \qquad (6)$$

where it has been assumed that $\partial T/\partial z = 0$ and $\rho = 0$ for $z = \infty$. It should be noted that equation (6) reduces to a very simple form when $\partial T/\partial z = 0$, i.e. at the mesopause

$$K = \frac{\int_{z'}^{\infty} (P - L)\, dz}{\rho g} \qquad (7)$$

Since $\int_{z'}^{\infty} P\, dz$ is the daily averaged heat input in a vertical column above height z' and since $\int_{z'}^{\infty} L\, dz$ is the daily averaged loss by radia-

tion in the same column, the eddy diffusion coefficient, when $\partial T/\partial z = 0$, can be considered as the ratio between the net energy input in a vertical column and the absolute value ρg of the atmospheric pressure gradient at the bottom of the column.

Application of expression (6) requires an atmospheric model, and the knowledge of heating and cooling rates. Incoherent scatter data are used in the following way. First the vertical temperature distribution is given by equation (3) for solstice and equinox conditions. The corresponding molecular nitrogen concentration at 95 km is used to compute a molecular nitrogen distribution between 95 and 120 km. Atomic and molecular oxygen concentrations are computed at each height by taking rations $n(O)/n(N_2)$ and $n(O_2)/n(N_2)$ identical to the ratios in the U.S. Standard Atmosphere (1976). Such an approximate procedure is adopted since O and O_2 are far from being in diffusive or in mixing equilibrium between 95 and 120 km. The O_2 distribution is then used for the computation of the solar heating rates in the Herzberg continuum, in the Schumann-Runge bands and in the Schumann-Runge continuum with help of the parameterized expressions developed by Strobel (1978). The almost negligible contribution due to ozone is also taken from Strobel (1978). All these instantaneous heating rate are integrated over a 24 hours period and a subsequent vertical integration leads to $\int_{z'}^{\infty} P\, dz$. The effective integrated heat input above 120 km for wavelengths shorter than 1250 Å must be added to the integrated heat input resulting from O_2 and O_3 between 95 and 120 km. Amayenc, Alcaydé and Kockarts (1975) have shown that, for solar activity conditions corresponding to a solar decimetric flux of 125×10^{-22} W m^{-2} Hz^{-1}, a solar extreme ultraviolet energy flux of 1.7 erg cm^{-2} s^{-1} is converted into heat above 120 km. In the present computation, we adopt two extreme values of 1 and 2 erg cm^{-2} s^{-1} for overhead sun conditions.

Between 95 and 120 km, the major cooling rate results from the 15 μm infrared band of CO_2. The expression for the cooling rate is taken from Houghton (1969) with a relaxation of 3×10^{-5}s at 1 atmosphere pressure in agreement with the low temperature measurements of Simpson, Gait and Simmie (1977). The vertical distribution of CO_2 simultaneously depends on the molecular diffusion coefficient taken from Banks and Kockarts (1973) and on the unknown eddy diffusion coefficient. Equation (6) is therefore solved by an iterative process in which the CO_2 distribution is computed with the formalism given by Kockarts (1973).

The eddy diffusion coefficients obtained in such a way are shown on Fig. 9 for spring, summer and winter conditions above Saint-Santin. For each season, the two curves respectively correspond to an overhead solar heat input of 1 and 2 erg cm^{-2} s^{-1} above 120 km altitude. Such an arbitrary variation indicates the possible range for the diurnally averaged eddy diffusion coefficient. Furthermore, a definite seasonal variation is apparent on Fig. 9. The winter lower thermosphere is much less turbulent than the summer one, since there is a smaller amount of heat to be transported downwards by turbulent conduction during winter. The seasonal variation shown on Fig. 9 contributes significantly to the helium winter bulge observed at higher altitude (see Kockarts, 1972; 1973). It is actually a complementary mechanism to the meridional circulation mechanism initially introduced by Johnson and Gottlieb (1970). A complete study of seasonal-latitudinal variations in the upper thermosphere should take into account simultaneously seasonal-latitudinal variations of the eddy diffusion coefficient in the lower thermosphere and meridional circulation. More experimental data are, however, needed to construct a global model for the eddy diffusion coefficient in the lower thermosphere.

It is interesting to evaluate the importance of the measured temperature distribution on the determination eddy diffusion coefficient.

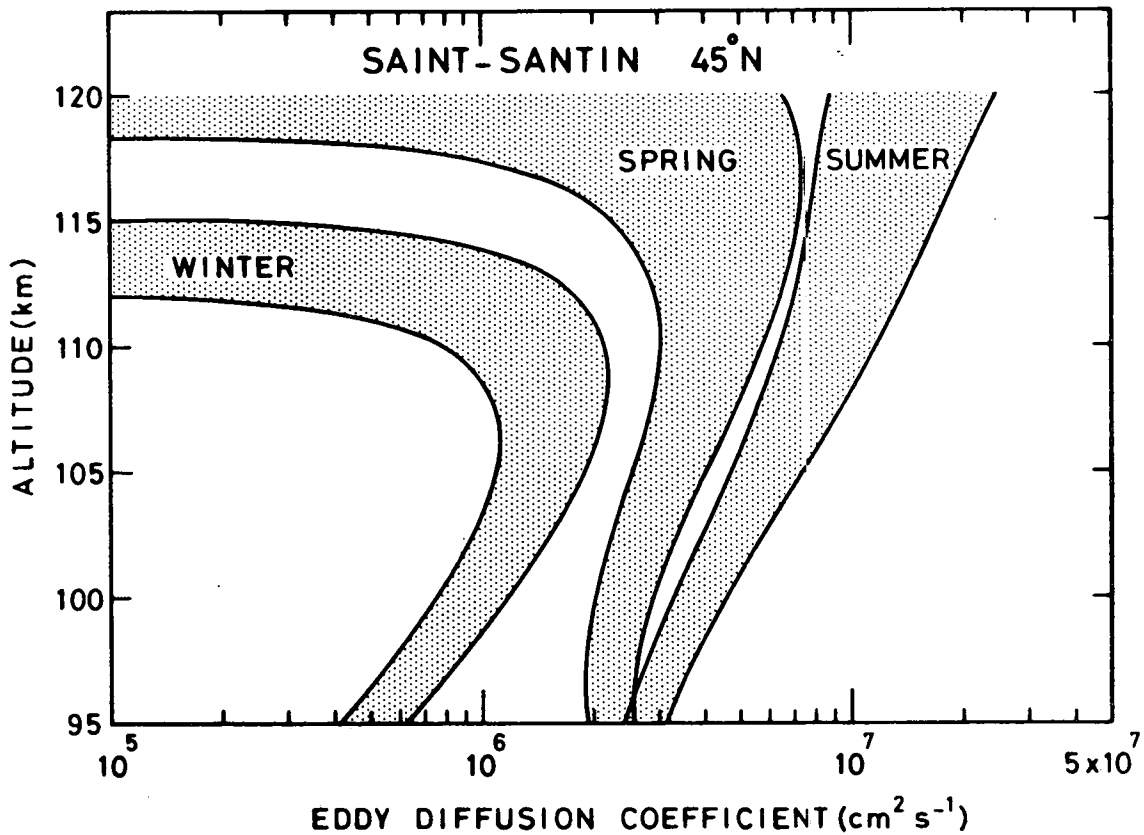

Fig. 9.- Vertical distribution of eddy diffusion coefficients for winter, spring and summer conditions. For each season the low values correspond to an overhead heat input of 1 erg cm^{-2} s^{-1} above 120 km and the high values correspond to 2 erg cm^{-2} s^{-1}.

Fig. 10 shows a comparison of the eddy diffusion coefficient obtained with the incoherent scatter temperature profiles and the empirical profile of Jacchia (1977). The overhead solar heat input above 120 km is 1.5 erg cm^{-2} s^{-1}, i.e. a value intermediate between the values used in Fig. 9. It appears that the Jacchia's profiles and the incoherent scatter profiles lead to similar eddy diffusion coefficients except at 120 km for equinox conditions. Expression (6) indicates that such differences result essentially from the underestimation of the temperature gradient at 120 km in the model of Jacchia (1977). Such an example shows the need for a good knowledge of the temperature gradient to achieve an accurate determination of the eddy diffusion coefficient. However, other factors such as the production and loss terms are equally important although they are not accessible through the incoherent scatter technique.

5. CONCLUSIONS

Incoherent scatter observations of ion temperature and ion-neutral collision frequencies allowed the evaluation of the neutral temperature in the 95-150 km altitude range and of the molecular nitrogen concentrations between 95 and 110 km. The data gathered over St-Santin during the last solar cycle were analytically adjusted in order to get a long term modelling of these parameters. This analysis shows that above the 100 km level, where the mean diurnal temperature is nearly constant, the seasonal effect increases with altitude while the semi-annual effect is weak. For molecular nitrogen concentrations the main component is semi-annual at 95 km and annual at 100 km and above. Special focus has been put on the E region where the characteristic temperatures issued from the Fourier modelling are adjusted by a quadratic dependence with altitude. Assuming that molecular nitrogen is in mixing

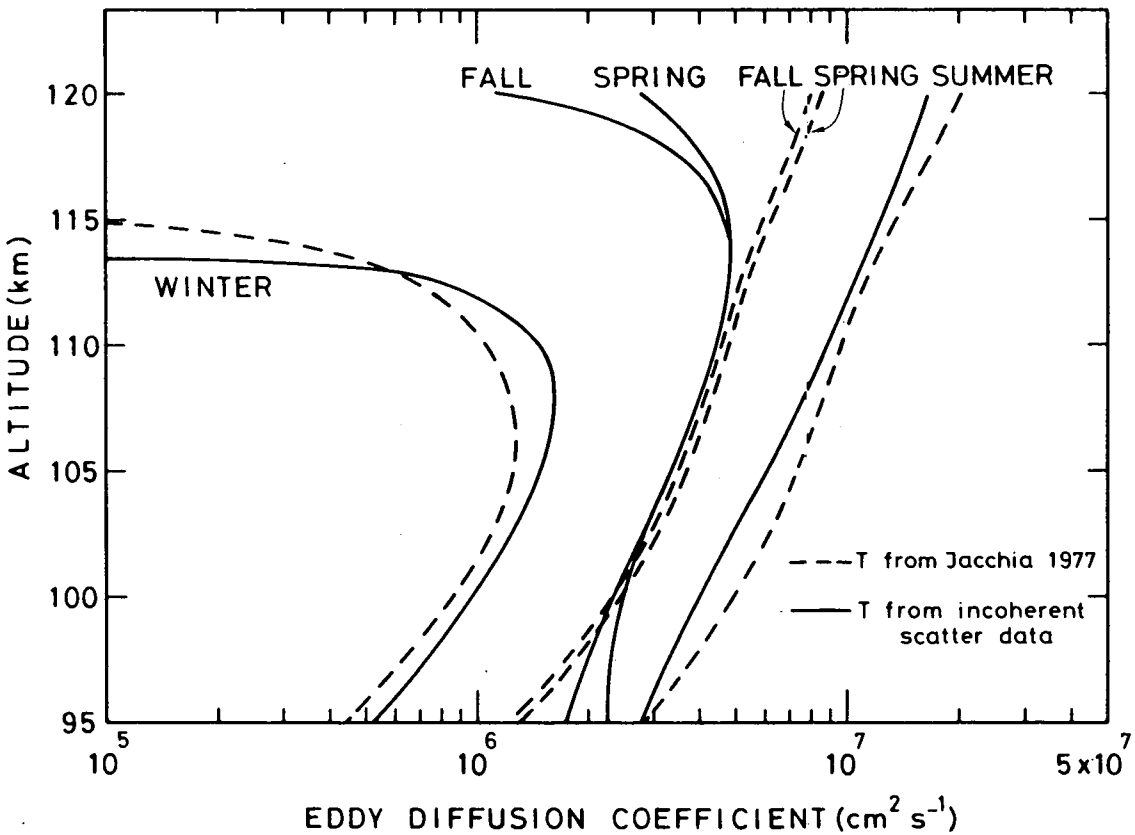

Fig. 10.- Comparison between eddy diffusion coefficients respectively obtained with the incoherent scatter temperature profiles (full curves) and the Jacchia's (1977) temperature profile (dashed curves). The overhead heat input above 120 km is 1.5 erg cm^{-2} s^{-1}.

equilibrium, one has shown that the vertical decrease of the concentrations according to the observed temperatures is consistent with the observed concentrations for each seasons, except at 110 km where various effects lead to an overestimation of the N_2 concentration.

Using the incoherent scatter temperature modelling and theoretical estimates for the heat production and loss rates, it has been possible to evaluate vertical profiles of the eddy diffusion coefficient between 95 km and 120 km altitude. Diurnally averaged eddy diffusion coefficients are obtained under the assumption that a turbulent downward heat transport is required to eliminate the excess heat input resulting from the imbalance between heat production, downward molecular heat conduction and infrared loss. The results show a large seasonal variation with small values during winter and large values during summer. Furthermore, it appears that the turbopause height is at lower altitudes during winter than at the equinoxes and at the summer solstice. It must be realized, however, that large uncertainties can affect the results on Figs. 9 and 10 since the production and loss terms depend on numerous parameters. Nevertheless, the general trend shown on Figs. 9 and 10 significantly contributes to the existence of the winter helium bulge and the summer argon bulge observed in the thermosphere.

The present analysis is actually intended as a constribution to the effort of a global modellization of the lower thermosphere where more experimental data are still needed.

ACKNOWLEDGEMENT

We gratefully acknowledge the contribution of Christine Mazaudier (CRPE) in the computation of the biasing effect of rapidly varying geophysical parameters over the observing volume investigated by the incoherent scatter technique. The valuable programming help of Emile Falise (IAS) is also greatly appreciated.

REFERENCES

ALCAYDE, D., P. BAUER and J. FONTANARI, Long-term variation of thermospheric temperature and composition, J. Geophys. Res., 79, 629-637, 1974.

ALCAYDE, D., P. BAUER, A.E. HEDIN and J.E. SALAH, Compatibility of seasonal variations in midlatitude thermospheric models at solar maximum and low geomagnetic activity, J. Geophys. Res., 83, 1141-1144, 1978.

AMAYENC, P., D. ALCAYDE and G. KOCKARTS, Solar extreme ultraviolet heating and dynamical processes in the mid-latitude thermosphere, J. Geophys. Res., 80, 2887-2891, 1975.

BANKS, P.M. and G. KOCKARTS, Aeronomy Part B, Academic Press, New York, 1973.

BERNARD, R., Tides in the E- region observed by incoherent scatter over Saint-Santin, J. Atmos. Terr. Phys., 36, 1105-1120, 1974.

BERNARD, R. and A. SPIZZICHINO, Semi-diurnal wind and temperature oscillation in the E- region observed by the Nançay incoherent scatter experiment, J. Atmos. Terr. Phys., 33, 1345-1352, 1971.

BLAMONT, J.E. and J. BARAT, Introduction d'un modèle pour la structure des mouvements de l'atmosphère entre 85 et 110 km d'altitude, Ann. Géophys., 23, 173-195, 1967.

DOUGHERTY, J.P. and D.T. Jr. FARLEY, A theory of incoherent scattering of radio waves by a plasma, 3. Scattering in a partly ionized gas, J. Geophys. Res., 68, 5473-5486, 1963.

FONTANARI, J. and D. ALCAYDE, Observation of neutral temperature tidal type oscillations in the F_1 region, Radio Sci., 9, 275-280, 1974.

HARPER, R.M., Tidal winds in the 100 to 200 km region at Arecibo, J. Geophys. Res., 82, 3243-3250, 1977.

HOUGHTON, J.T., Absorption and emission by carbon dioxide in the mesosphere, Quart. J. Roy. Met. Soc., 95, 1-20, 1969.

HUNTEN, D.M., Energetics of thermospheric eddy transport, J. Geophys. Res., 79, 2533-2534, 1974.

IZAKOV, M.N., Effect of turbulence on the thermal regime of planetary thermospheres, Kosmicheskie Issledovaniya, 16, 403, 1978.

JACCHIA, L.G., Revised static models of the thermosphere and exosphere with empirical temperature profiles, Smith. Astrophys. Obs. Special Report n° 332, 1971.

JACCHIA, L.G., Thermospheric temperature, density, and composition : new models, Smith. Astrophys. Obs. Special Report n° 375, 1977.

JOHNSON, F.S., Transport processes in the upper atmosphere, J. Atmos. Sci., 32, 1658-1662, 1975.

JOHNSON, F.S. and B. GOTTLIEB, Eddy mixing and circulation at ionospheric levels, Planet. Space Sci., 18, 1707-1718, 1970.

JOHNSON, F.S. and E.M. WILKINS, Thermal upper limit on eddy diffusion in the mesosphere and lower thermosphere, J. Geophys. Res., 70, 1281-1284, 1965a.

JOHNSON, F.S. and E.M. WILKINS, Correction to "Thermal upper limit on eddy diffusion in the mesosphere and lower thermosphere", J. Geophys. Res., 70, 4063, 1965b.

KOCKARTS, G., Distribution of hydrogen and helium in the upper atmosphere, J. Atmos. Terr. Phys., 34, 1729-1743, 1972.

KOCKARTS, G., Helium in the terrestrial atmosphere, Space Sci. Rev., 14, 723-757, 1973.

MATHEWS, J.D., Measurements of the diurnal tides in the 80 to 100 km altitude range at Arecibo, J. Geophys. Res., 81, 4671-4677, 1976.

PHILBRICK, C.R., G.A. FAUCHER and E. TRZCINSKI, Rocket measurements of mesospheric and lower thermospheric composition. Space Research XIII, Akademie-Verlag, Berlin, 256-260, 1973.

SALAH, J.E., Daily oscillations of the mid-latitude thermosphere studied by incoherent scatter of Millstone Hill, J. Atmos. Terr. Phys., 36, 1891-1909, 1974.

SALAH, J.E., J.V. EVANS and R.H. WAND, Seasonal variations in the thermosphere above Millstone Hill, Radio Sci., 9, 231-238, 1974.

SALAH, J.E. and R. WAND, Tides in the temperature of the thermosphere at mid-latitude, J. Geophys. Res., 79, 4295-4304, 1974.

SIMPSON, C.J.S.M., P.D. GAIT and J.M. SIMMIE, The vibrational deactivation of the bending mode of CO_2 by O_2 and by N_2, Chem. Phys. Letters, 47, 133-136, 1977.

STROBEL, D.F., Parametrization of the atmospheric heating rate from 15 to 120 km due to O_2 and O_3 absorption of solar radiation, J. Geophys. Res., 83, 6225-6230, 1978.

TEITELBAUM, H. and J.E. BLAMONT, Variations of the turbopause altitude during the night, Planet. Space Sci., 25, 723-734, 1977.

TEPLEY, C.A. and J.D. MATHEWS, Preliminary measurements of ion-neutral collision frequencies and mean temperature in the Arecibo 80 - 100 km altitude region, J. Geophys. Res., 83, 3299-3302, 1978.

U.S. Standard Atmosphere 1976, U.S. Government Printing Office, Washington D.C., 1976.

VIDAL-MADJAR, D., Gravity wave detection in the lower thermosphere with the French incoherent scatter facility, J. Atmos. Terr. Phys., 40, 685-689, 1978.

WALDTEUFEL, P., Valeur et variation diurne de la densité atmosphérique à 100 km d'altitude, Planet. Space Sci., 17, 725-730, 1969.

WALDTEUGEL, P., A study of seasonal changes in the lower thermosphere and their implications, Planet. Space Sci., 18, 741-748, 1970.

WALDTEUFEL, P. and L. COGGER, Measurement of the neutral temperature at Arecibo, J. Geophys. Res., 76, 5322-5336, 1971.

WAND, R.H., Evidence for reversible heating in the E- region from radar Thomson scatter, J. Geophys. Res., 74, 5688-5696, 1969.

ZIMMERMAN, S.P. and F.A. MURPHY, Stratospheric and mesospheric turbulence, pp. 35-47 in Grandal, B. and J.A. Holtet (eds.) Dynamical and chemical coupling between neutral and ionized atmosphere, D. Reidel, Dordrecht, Holland, 1977.

ZIMMERMAN, S.P. and C.A. TROWBRIDGE, The measurement of turbulent spectra and diffusion coefficients in the altitude region 95 to ~ 110 km, Space Research XIII, Akademie-Verlag, Berlin, 203-208, 1973.